

Modeling of Nondirected Wireless Infrared Channels

Jeffrey B. Carruthers, *Member, IEEE*, and Joseph M. Kahn, *Member, IEEE*

Abstract—We show that realistic multipath infrared channels can be characterized well by only two parameters: optical path loss and rms delay spread. Functional models for the impulse response, based on infrared reflection properties, are proposed and analyzed. Using the ceiling-bounce functional model, we develop a computationally efficient method to predict the path loss and multipath power requirement of diffuse links based on the locations of the transmitter and receiver within a room. Use of our model is a simple, yet accurate, alternative to the use of an ensemble of measured channel responses in evaluating the impact of multipath distortion.

Index Terms—Indoor communication, multipath channels, optical communication.

I. INTRODUCTION

NONDIRECTED infrared light transmission with intensity modulation and direct detection (IM/DD) is a candidate for high-speed wireless communication within buildings. Characterization of this infrared channel has been performed using experimental measurements [1], [2] and simulation through ray-tracing techniques [3], which both have drawbacks as the primary technique for modeling. The results of experimental studies of the channel are highly dependent on the rooms selected for the measurement study, and it is not clear how to extend the results so obtained to other situations. Also, it is only possible to publish a small fraction of all of the measured channels or some summaries of their behavior, and hence it is difficult either to reproduce reported results that rely on such data or to use the data for further study. Ray tracing combined with simulation [3], [4] is computationally intensive.

This paper seeks to improve infrared channel characterization in two steps. First, we show that there exist simple functional forms for the impulse response that can reproduce the behavior of the measured channels. Second, we develop a simple model using these functions that takes account of room properties to predict the power requirements of links transmitting over multipath channels. In Section II, we review the infrared channel, and show how its differences from multipath fading radio channels suggest a different approach to modeling. Section III shows how the channels can be characterized by their delay spreads and optical path losses, and Section IV illustrates that these two parameters

Paper approved by M. S. Goodman, the Editor for Optical Switching of the IEEE Communications Society. Manuscript received April 15, 1996; revised March 20, 1997. This work was supported by the National Science Foundation under Grant ECS-9408957. This paper was presented in part at IEEE ICC'96, Dallas, TX.

J. B. Carruthers is with the Department of Electrical and Computer Engineering, Boston University, Boston, MA 02215 USA.

J. M. Kahn is with the Department of Electrical Engineering and Computer Sciences, University of California at Berkeley, Berkeley, CA 94720 USA.

Publisher Item Identifier S 0090-6778(97)07283-8.

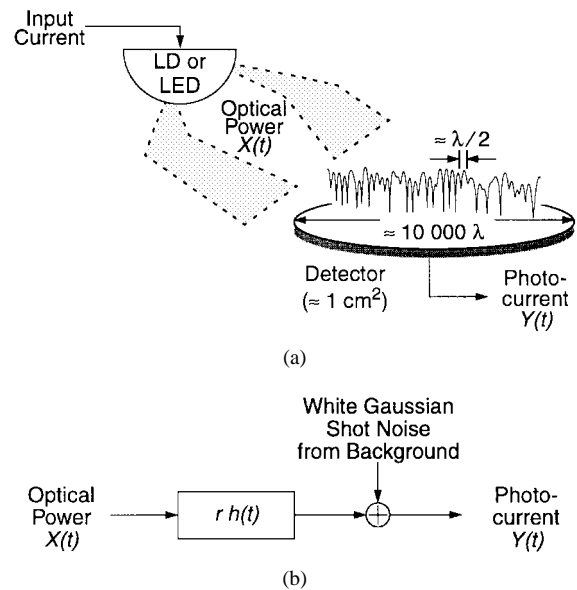


Fig. 1. Modeling nondirected infrared channels with intensity modulation and direct detection. (a) The photocurrent is proportional to the integral over the detector surface of the optical power. (b) The channel can be modeled as a fixed, linear, baseband system with input $X(t)$, output $Y(t)$, impulse response $h(t)$, and additive white, Gaussian noise.

are sufficient for estimating link power requirements. The functional model for the IM/DD channel is developed in Section V. A method for predicting power requirements of diffuse links based on the positions of the transmitter and receiver is given in Section VI, and Section VII presents some concluding remarks.

II. INTENSITY MODULATION/DIRECT DETECTION CHANNELS

The nondirected, infrared channel using intensity modulation with direct detection is depicted in Fig. 1. It comprises an infrared emitter as the transmitter and a large-area photodetector as the receiver. The input signal $X(t)$ is the instantaneous optical power of the emitter, and the output of the channel $Y(t)$ is the instantaneous current in the receiving photodetector, which is the product of the photodetector responsivity r and the integral over the photodetector surface of the instantaneous optical power at each location. The signal propagates to the receiver through a room with reflective surfaces. The channel can be modeled as a baseband linear system, with input power $X(t)$, output current $Y(t)$, and an impulse response $h(t)$, which is fixed for a certain physical configuration of receiver, reflectors, and transmitter [1]. The impulse response is quasistatic due to the high signaling rates, high-order diversity of the large-area receiver, and the low speeds at which indoor objects move. We assume that the links are operated

in the presence of intense infrared and visible background light, which results in additive, white, nearly Gaussian shot noise $n(t)$ that is the limiting factor in the signal-to-noise ratio (SNR) of a well-designed receiver. Our channel model is summarized by

$$Y(t) = rX(t) \otimes h(t) + n(t) \quad (1)$$

where \otimes denotes convolution.

Baseband models of indoor radio channels often consider impulse responses of the form

$$h(t) = \sum_{n=1}^N a_n \delta(t - t_n) e^{j\theta_n t} \quad (2)$$

where a_n, t_n, θ_n and N are statistically characterized [5]. The use of a δ -function as the base-modeling function is appropriate in the radio environment, where reflecting elements typically produce specular reflections. However, reflection of infrared radiation (and, indeed, visible light) by most surfaces in typical rooms is predominantly diffuse [6], i.e., the reflected light is scattered into a continuous distribution of angles, which is nearly independent of the incident angle. Hence, when a reflecting object is illuminated by the transmitter and this object lies in the receiver field of view, the result is a pulse extended in time. This leads us to consider for the base-modeling function some pulse shape $f(t)$ whose duration and shape correspond to the response produced by diffuse reflectors.

III. CHARACTERIZING INFRARED CHANNELS

The goal of characterizing a particular multipath infrared channel is to determine the average transmitted optical power

$$P_{tx} = \lim_{T \rightarrow \infty} \frac{1}{2T} \int_{-T}^T X(t) dt \quad (3)$$

required to achieve a certain bit-error rate for a particular modulation scheme. We separate the power requirements into two factors: an optical path loss and a multipath power requirement.

Defining the optical gain G_o for a channel with impulse response $h(t)$ to be $G_o = \int_{-\infty}^{\infty} h(t) dt$, then the received optical power is $P_{rx} = G_o P_{tx}$. Hence,

$$\text{optical path loss (optical dB)} = -10 \log_{10} G_o. \quad (4)$$

We will show that a single parameter of the channel impulse response, the normalized delay spread, is an excellent predictor of the multipath power requirement. Let us define a function $P(\text{BER}, h(t), N_0, \text{MS})$ as the average optical transmitted power required when using the modulation scheme MS to achieve a bit-error rate of BER over the channel with impulse response $h(t)$ in the presence of additive white Gaussian noise of power-spectral density N_0 . Then the *normalized power requirement* is

$$\frac{P_{\text{avg}}}{P_{\text{OOK}}} = \frac{P(\text{BER}, h(t)/G_o, N_0, \text{MS})}{P(\text{BER}, \delta(t), N_0, \text{OOK})} \quad (5)$$

which can be thought of as a power penalty for the modulation scheme and channel compared to on-off keying (OOK) on a

nondistorting channel. Since the channels $h(t)/G_o$ and $\delta(t)$ have the same optical path loss, only the effect of the multipath dispersion is measured. In this paper, the power requirements are calculated for $\text{BER} = 10^{-9}$.

The temporal dispersion of an impulse response $h(t)$ can be expressed by the *channel rms delay spread* D , which is calculated from the impulse response according to

$$D = \left[\frac{\int (t - \mu)^2 h^2(t) dt}{\int h^2(t) dt} \right]^{1/2} \quad (6)$$

where the mean delay μ is given by

$$\mu = \left(\int t h^2(t) dt \right) / \left(\int h^2(t) dt \right) \quad (7)$$

and the limits of integration in (6) and (7) extend over all time. We emphasize that since $h(t)$ is fixed for a given configuration, so is the rms delay spread. The *normalized delay spread* D_T is a dimensionless parameter defined as the rms delay spread D divided by the bit duration T .

IV. POWER REQUIREMENT AND DELAY SPREAD

In this section, we investigate the relationship between the normalized delay spread D_T and the multipath power requirement $P_{\text{avg}}/P_{\text{OOK}}$ for three classes of modulation schemes: on-off keying (OOK), pulse-position modulation (PPM), and multiple-subcarrier modulation (MSM).

The channels considered have been measured in two studies [1], [7]. In the first study, 80 channels from various locations in five offices were studied. These include LOS configurations (transmitter placed at the ceiling and pointed down) and diffuse configurations (transmitter placed at desk height and pointed up), and some of the channels were shadowed (by a person standing next to the receiver). During all measurements, the receiver was placed at desk height and pointed upward. The transmitter was approximately Lambertian of order 1, i.e., with angular irradiance proportional to the cosine of the angle with respect to the transmitter normal. The second study investigated 26 diffuse channels in a single large room, and here the transmitter used is approximated by a generalized Lambertian [6] of order 1.85, i.e., with angular irradiance proportional to the 1.85th power of the cosine of the angle with respect to the transmitter normal.

A. On-Off Keying

We consider power requirements for baseband OOK at bit rates of 30, 55, and 100 Mbits/s with three detection methods: unequalized, equalized using a zero-forcing decision-feedback equalizer (ZF-DFE), and maximum likelihood sequence detection (MLSD). The transmitter encodes a one in a rectangular pulse of duration T , where $1/T$ is the bit rate. For unequalized operation, the receiver filter is a five-pole Bessel receiver filter having a 3-dB cutoff frequency $0.6/T$, and for ZF-DFE, the same filter is employed, but with a cutoff frequency of $0.45/T$. These receive filters have been found to perform better than rectangular impulse-response filters [1], and their

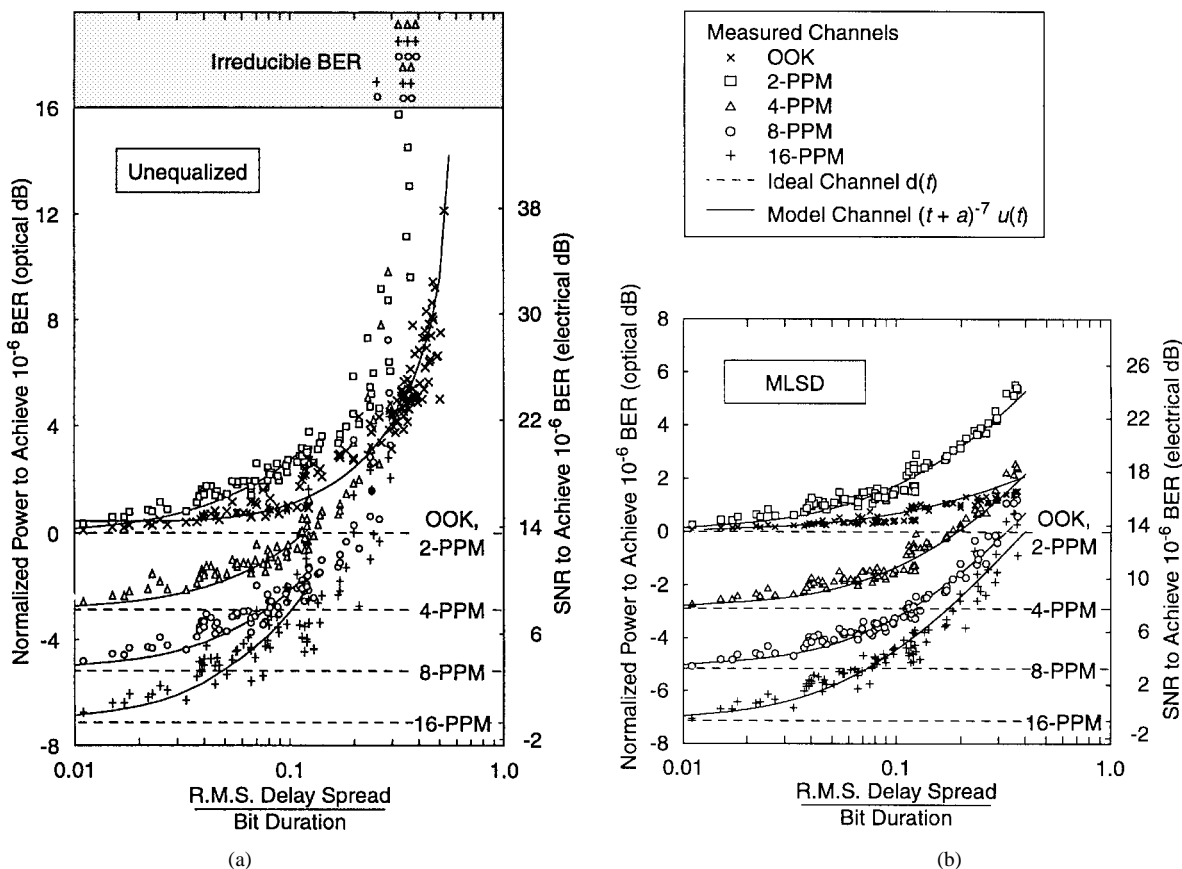


Fig. 2. Dependence of (a) unequaled multipath power requirements and (b) maximum-likelihood sequence-detection multipath power requirements on the normalized delay spread for on-off keying and pulse-position modulation. The scatter plots show the power requirements for measured diffuse and LOS channels for 10, 30, 55, and 100 Mbits/s, and the lines show the relationship between power requirement and delay spread for channel impulse responses of the form $u(t)/(t+a)^7$. All power requirements are relative to the power required by OOK on a nondistorting channel having the same optical path loss as the multipath channel.

cutoff frequencies have been chosen to provide optimum performance with measured channel responses. For MLSD detection, the optimal whitened-matched filter is used.

Fig. 2(a) illustrates that any two measured channels with the same D_T have unequaled power requirements that closely agree, and likewise, Fig. 2(b) shows that their MLSD power requirements closely agree. Further, we see the effectiveness of normalizing the delay spread to the bit duration, as the power requirements at different bit rates nearly coincide when expressed as a function of the normalized delay spread. The unequaled power requirements (in decibels) increase exponentially to about 13 dB for $D_T = 0.5$. For $D_T > 0.55$, most measured channels cannot achieve the target BER of 10^{-9} due to the severity of the intersymbol interference. The MLSD power requirements (in decibels) increase approximately quadratically with normalized delay spread to about 2 dB for $D_T = 0.3$, and the power requirements using a ZF-DFE are within 0.1 dB of MLSD in that range of delay spreads.

B. Pulse-Position Modulation

Fig. 2 shows the relationship between D_T and power requirement for L -position PPM (L -PPM), where L is one of 2, 4, 8, or 16. The transmit pulse and the receive filter are both rectangular. The bit rates considered are 10 and 30 Mbits/s, and we consider both unequaled operation and MLSD [8]. The

multipath power requirement of PPM is very well predicted by D_T for measured channels, particularly for 2-, 4-, and 8-PPM.

C. Multiple-Subcarrier Modulation

Fig. 3 shows the relationship between D_T and power requirement for a link using two subcarriers, each using 4-QAM modulation. The subcarrier center frequencies are $1/(4T)$ and $3/(4T)$ where $1/4T$ is the symbol rate and so $1/T$ is the bit rate. The bit rates considered are 30, 55, and 100 Mbits/s, and pulses having a root-raised-cosine Fourier transform with 100% excess bandwidth are used. We note that delay spread is not a reliable predictor of the power requirement for multiple-subcarrier modulation: the power requirement varies up to about 4 dB for a given D_T .

V. FUNCTIONAL MODELING OF MULTIPATH DISPERSION

While the relationship between power requirement and delay spread is interesting, it does not by itself eliminate the need to evaluate a modulation scheme over an entire ensemble of channels and over the range of applicable bit rates. This motivates us to look for simple functional forms for $h(t)$ that exhibit the same relationship between power requirement and delay spread as do the measured channels, and hence can be used in the place of measured channel

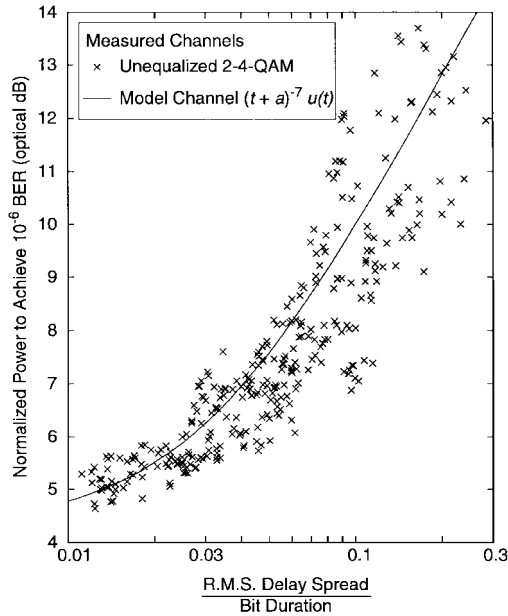


Fig. 3. Dependence of unequalized multipath power requirements on the normalized delay spread, for multiple-subcarrier modulation. Two 4-QAM subcarriers are employed. The scatter plots show the power requirements for measured diffuse and LOS channels for 30, 55, and 100 Mbits/s. The line shows the relationship between power requirement and delay spread for channel impulse responses of the form $u(t)/(t+a)^7$. The power normalization is as in Fig. 2.

ensembles in performance evaluation. In keeping with our separation of the effects of path loss and multipath, we will set $G_o = \int h(t) dt = 1$ for candidate modeling impulse responses $h(t)$.

A. Exponential-Decay Model

There are two physical processes that produce multipath dispersion observed in diffuse IM/DD channels, and that lead us to consider candidate functional forms for $h(t)$. The first such process is multiple reflections. The light captured by the receiver can be partitioned according to the number of surfaces off which it has reflected [3], i.e., there is light coming directly from the transmitter, light arriving after a single reflection, and so on. Since each surface has a reflectivity less than one, then one might expect the power received from $n+1$ bounces to be less than that received from n bounces by a factor of R , the average reflectivity of the surfaces in the room. Further, the time of arrival of bounce $n+1$ is delayed by a certain time from the arrival of bounce n . Hence, according to this model, the channel impulse response would be a sequence of delta functions whose amplitudes decay geometrically. This geometric series is very similar to a decaying exponential impulse response

$$h_e(t, \tau) = \frac{1}{\tau} \exp(-t/\tau) u(t) \quad (8)$$

which defines the *exponential-decay model* for multipath dispersion. It will be used rather than a geometric-series model as it is simpler to express and also takes into account the second dispersive influence on the impulse response, diffuse reflection. The delay spread and 3-dB cutoff frequency for the

exponential-decay model are given by the following relations:

$$D(h_e(t, \tau)) = \tau/2 \quad (9)$$

$$f_{3\text{ dB}}(h_e(t, \tau)) = \frac{1}{4\pi D(h_e(t, \tau))}. \quad (10)$$

B. Ceiling-Bounce Model

The impulse response due to diffuse reflection from a single infinite-plane reflector will be used as a second candidate form for $h(t)$. The infinite Lambertian-reflecting plane is chosen, as it is a good approximation to a large ceiling. The general form of the impulse response is derived in the Appendix, and a closed-form solution (33) is given for the case in which the horizontal separation of the transmitter and receiver is zero. This expression is rather cumbersome, and for the purpose of developing a simple base model function, we make the further assumption that the transmitter and receiver have the same separation from the ceiling (and hence are colocated).

Setting $l = 0$ in (33) so that the receiver and transmitter are colocated yields

$$h(t) = \frac{c\rho AH^4}{\pi} \frac{ct}{2} u\left(t - \frac{2H}{c}\right) = \frac{2^7 \rho AH^4}{c^6 \pi t^7} u\left(t - \frac{2H}{c}\right) \quad (11)$$

where ρ is the plane reflectivity, A is the receiver photodiode area, and H is the height of the ceiling above the transmitter and receiver.

The minimum time required for a signal to travel from the transmitter, reflect off the ceiling, and then strike the receiver is $2H/c$. For consistency with the exponential decay model, we eliminate this delay by shifting the time origin in (11) by $2H/c$ to obtain

$$h(t) = \frac{\rho A}{3\pi H^2} \frac{6(2H/c)^6}{(t + 2H/c)^7} u(t) \quad (12)$$

where the constants have been rearranged so that the factor $\rho A/(3\pi H^2) = G_o$. Let $a = 2H/c$, and assume $G_o = 1$, then we have

$$h_c(t, a) = \frac{6a^6}{(t+a)^7} u(t) \quad (13)$$

which defines the *ceiling-bounce model* for multipath dispersion. The delay spread and 3-dB cutoff frequency for the ceiling-bounce model are given by the following relations:

$$D(h_c(t, a)) = \frac{a}{12} \sqrt{\frac{13}{11}} \quad (14)$$

$$f_{3\text{ dB}}(h_c(t, a)) = \frac{K}{4\pi D(h_c(t, a))} \quad (15)$$

where K is given by

$$\left| \int_0^\infty \frac{\exp(-j \cdot 6Ku\sqrt{11/13})}{(1+u)^7} du \right| = \frac{1}{6\sqrt{2}} \quad (16)$$

and is approximately 0.925. We see by comparing (15) with (10) that the ceiling-bounce response exhibits the same reciprocal relationship between delay spread and 3-dB cutoff

frequency as does the exponential decay response, but exhibits a slightly smaller 3-dB cutoff frequency for the same delay spread.

C. Agreement with Measured Channels

We show that the functional models developed previously accurately reproduce the relationship between delay spread and multipath power requirement exhibited by measured channels. Although the exponential-decay and ceiling-bounce models correspond most closely with LOS and diffuse channels, respectively, we will see that they accurately model the relationship between delay spread and multipath power requirement for all four types of channels considered—LOS shadowed and unshadowed, and diffuse shadowed and unshadowed.

The loci of power requirements generated by $h_c(t, a)$ by varying the parameter a , and hence also the delay spread are shown in Figs. 2 and 3. Although the decaying exponential impulse response produced curves similar to the ceiling-bounce function, the fit to the experimental data was inferior. For both the ceiling-bounce model and the exponential-decay model, the standard deviation of the difference between the measured power requirement and the modeled power requirement was 0.9 dB (unequalized OOK) and 0.2 dB (OOK with MLS). However, the mean difference was 0.1 dB (unequalized OOK) and 0.2 dB (OOK with MLS) for the exponential decay model, whereas these mean differences were less than 0.1 dB for the ceiling-bounce model. Hence, we use the ceiling-bounce model from here on, as it provides a slightly better fit to the measured channels. The exponential-decay model is also viable, and it does have the advantage of greater simplicity, and hence, tractability.

VI. MODELING DELAY SPREAD, POWER REQUIREMENT, AND PATH LOSS

We focus here on characterizing the impulse response of diffuse channels in actual rooms. The impulse response is assumed to be of the form

$$h(t) = G_o h_c(t, a) \quad (17)$$

where a and G_o are determined by the locations and orientations of the receiver and transmitter within the room (using a method we will now develop) and $h_c(t, a)$ is the ceiling-bounce impulse response. Referring to (13), in which we set $a = 2H/c$ to derive the ceiling-bounce model, we can think of $ac/2$ as the effective height of the ceiling above the transmitter and receiver.

The validity of our approach will be evaluated by its ability to accurately predict the actual path loss and multipath power requirement found for the experimental channels, and hence, the required transmit power to achieve the system performance requirements.

When the transmitter and receiver are near the center of a large room, and in a diffuse configuration, one expects the impulse response to be dominated by the impulse response due to a single bounce off the ceiling. When the receiver is further separated from the transmitter, two other effects come

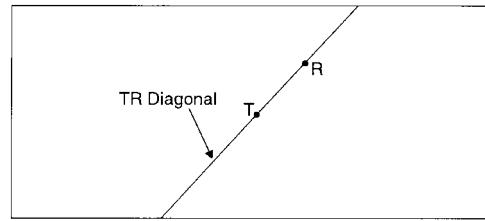


Fig. 4. Normalization of the room size is done through the use of the TR diagonal, defined as the length of that segment of the line TR between the transmitter and the receiver that lies within the room.

into play: the ceiling no longer appears to the transmitter to be well approximated by an infinite plane, and the contribution of the walls to the impulse response will increase relative to that of the ceiling. This leads us to consider the following two-stage modeling approach: a first-order approximation will be made assuming an infinitely large room, and a correction will be applied which takes into account position within the room. The parameter used for this correction will be the ratio of the horizontal separation of the transmitter and receiver to the TR diagonal, shown in Fig. 4. Note that this ratio does not account for the height of the transmitter or receiver, and hence results using this ratio may be valid only for heights similar to those in the measurement studies.

A. Estimation of the Ceiling-Bounce Parameter

As previously determined, the delay spread is a simple parameter that accurately predicts the multipath power requirement. Our strategy for selecting the ceiling-bounce parameter a , then, will rely on first accurately predicting the delay spread, and then setting a so that $D(h_c(t, a))$ matches the predicted delay spread.

In order to estimate the channel delay spread, we first compute the impulse response if one removed all the walls, and extended the ceiling infinitely in all directions. This “one-bounce impulse response” $h_1(t)$ is found through numerical integration of (28) for the actual locations of the transmitter, receiver, and the extended ceiling. While reflections from walls cause the delay spreads in finite-sized rooms to be larger than those predicted by the “one-bounce” model, we have found empirically that the increase on delay spread can be predicted approximately by a simple function of the ratio s of the horizontal transmitter–receiver separation to the TR diagonal. This is illustrated in Fig. 5.

For diffuse unshadowed channels, the increase in delay spread due to multiple bounces is well predicted by a quadratic function of s . The increase in delay spread ranges from a factor of 2 at small separations to about 5 at the edges of a room,¹ and we predict a using

$$a(\text{unshad.}) = 12\sqrt{11/13}(2.1 - 5.0s + 20.8s^2)D(h_1(t)), \quad (18)$$

For shadowed channels, the delay spreads are more variable, but still increase with separation. A linear fit is employed, as

¹Since the transmitter is at the center of the room, this corresponds to a separation-diagonal ratio of $s = 0.5$.

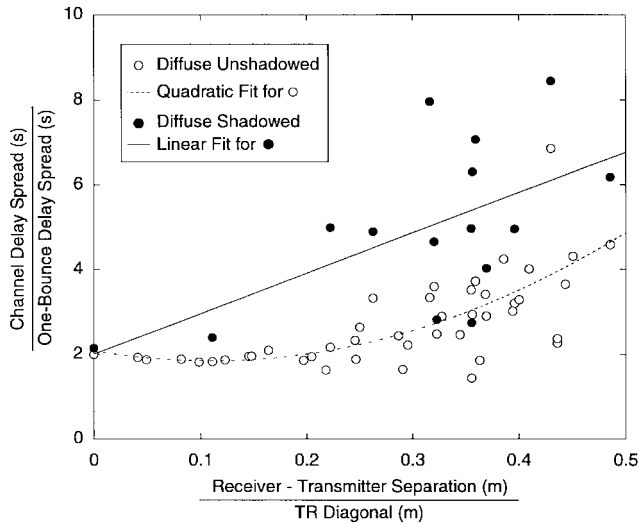


Fig. 5. Predicting delay spread from room location for diffuse channels. The ratio of the channel delay spread to the delay spread of the ceiling-only impulse response as a function of the ratio of the horizontal separation between the receiver and transmitter and the TR diagonal.

the data do not exhibit a clear enough pattern to justify fitting to a higher order curve. Hence, we predict a using

$$a(\text{shadowed}) = 12\sqrt{11/13}(2.0 + 9.4s)D(h_1(t)). \quad (19)$$

B. Multipath Power Requirement

We are now in a position to estimate the multipath power requirement using the ceiling-bounce parameter a estimated from (18) or (19), and the resulting estimated impulse response $G_o h_c(t, a)$. We consider the same OOK link parameters as in Section IV. The results of this estimation for diffuse shadowed and diffuse unshadowed channels are shown in Fig. 6. For unequalized OOK, the estimation of power requirement is within 1 dB of the power requirement computed using measured channel responses for 90% of the channels and within 2 dB for all channels. The estimation of power requirement when a ZF-DFE is employed is within 0.5 dB for 95% of the channels and within 1 dB for all channels.

C. Path Loss

We follow the same procedure used for predicting delay spread and the ceiling-bounce parameter. We first find the optical gain $G_o = \int h_1(t) dt$ of the impulse response $h_1(t)$ from a single bounce off the ceiling (infinitely extended, as before), and then adjust this value based on the position within the room using s , the ratio of the horizontal transmitter–receiver separation to the TR diagonal. In finite-sized rooms, the walls and floor will allow for multiple reflections to arrive at the receiver, and so we expect to see less path loss in such rooms than that predicted by the one-bounce impulse response. This reduction in path loss is especially evident when the receiver approaches a wall, and we will attempt to account for these effects using the ratio s .

In all six rooms from which measurements are used, the ceiling, of gray–white tile material, is approximately Lambertian-

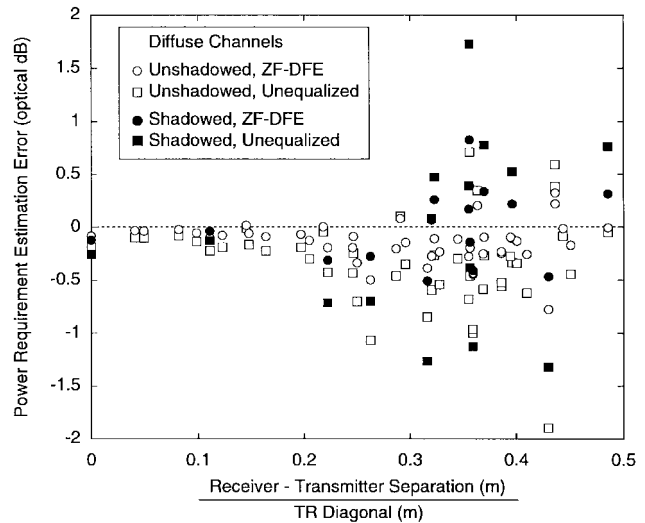


Fig. 6. Errors in estimating multipath power requirements (relative to the measured channels) as a function of the ratio of the horizontal separation between the receiver and transmitter normalized and the TR diagonal. This graph considers diffuse, unshadowed and diffuse, shadowed channels.

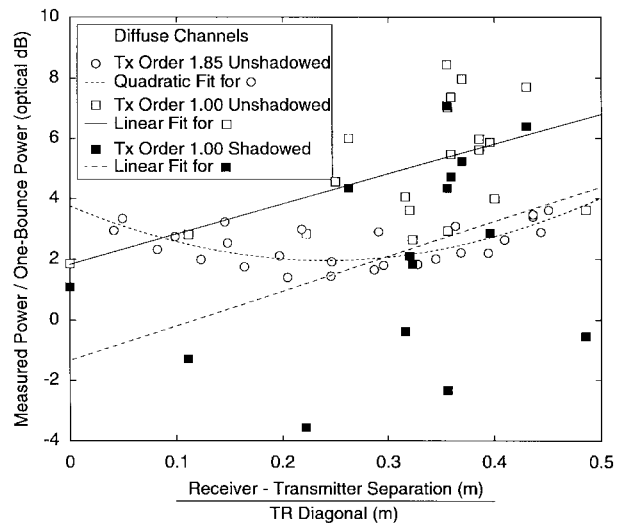


Fig. 7. Ratio of measured received optical power to power from one-bounce impulse response as a function of receiver location for diffuse channels. The effect of the directionality of the transmitted beam, as measured by the Lambertian order, is evident.

reflecting with a power reflectivity of about 0.65. Using this model for the ceiling, the predicted one-bounce path losses range from 55 to 71 dB for a photodiode area $A = 1 \text{ cm}^2$. For measured unshadowed channels, the received optical power ranges from 1 to 9 dB greater than the one-bounce power. For measured shadowed diffuse channels, the received optical power ranges from 7 greater to 4 dB less than the one-bounce power. Shadowed channels can receive less power than the predicted one-bounce power since the shadowing object is blocking part of the light traveling to the ceiling from the transmitter and also part of the light traveling from the ceiling to the receiver.

The use of the ratio s to adjust the one-bounce estimate of path loss is illustrated in Fig. 7, and the resulting prediction

of optical gains is summarized as follows:

$$\begin{aligned}
 G_o(\text{unshad.}, n = 1.85) &= 10^{0.37-1.20s+2.55s^2} \int h_1(t) dt \\
 G_o(\text{unshad.}, n = 1.00) &= 10^{0.18+1.00s} \int h_1(t) dt \\
 G_o(\text{shad.}, n = 1.00) &= 10^{-0.14+1.02s} \int h_1(t) dt.
 \end{aligned} \tag{20}$$

Here, the channels using an order-1.85 Lambertian transmitter exhibit different behavior from those using a Lambertian of order 1. The increased directionality of the order 1.85 source increases the effect of the contribution from a ceiling reflection, followed by a floor reflection, and then a second ceiling reflection. This is evidenced in the upturn of the measured power curves at small s for the more directional transmitter. Also, the additional power due to the walls and multiple bounces is smaller for the more directional transmitter at large separations.

D. Modeling LOS Channels

While LOS channels exhibit the same relationship between multipath power requirement and delay spread as diffuse channels, their parameters are less easily estimated than those of diffuse channels using simple characteristics of the room.

The LOS unshadowed channel can be modeled approximately by assuming that the LOS path dominates, and so the impulse response is [6]

$$h(t) = \frac{AH^2}{\pi L^4} \delta(t - L/c) \tag{21}$$

where H is the vertical separation between the transmitter and receiver and L is the straight-line separation. The source is a first-order Lambertian, the transmitter is pointed down, and the receiver is pointed up. Other arrangements would change the optical gain, which is $G_o = AH^2/(\pi L^4)$, but the delay spread would still be nearly zero as long as the LOS path dominates. However, typically, the optical gain is between 1 and 2 dB higher than this initial estimate (due to reflections), and this increase exhibits no apparent correlation with position within the room. Similarly, the delay spread, while typically less than 2 ns, also exhibits no apparent correlation with position within the room.

LOS shadowed channels are even more difficult to model. Since the LOS path is blocked, the entire response is determined by reflections which, as for LOS unshadowed channels, are unpredictable. Hence, neither the path loss nor the delay spread is easily predicted. However, as LOS shadowed channels tend to have high path loss and large delay spreads [1], they are generally unacceptable anyway.

VII. CONCLUSIONS

We have shown that nondirected IM/DD channels can be well characterized solely by their path loss and delay spread. This is due to the strong correlation between multipath power requirement and delay spread for baseband modulation

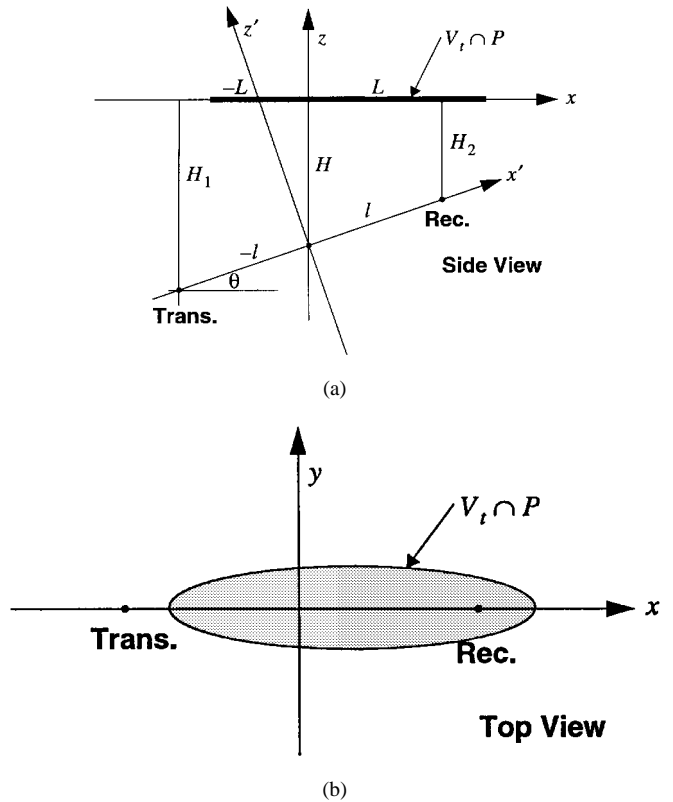


Fig. 8. Geometry of transmitter, ceiling plane P , and receiver. The transmitter is located at $(-L, 0, -H_1)$ and the receiver is at $(+L, 0, -H_2)$. The surface $V_t \cap P$ is the part of the ceiling contributing to the impulse response in the interval $[0, t)$, and is the interior of an ellipse. The drawing is for $H_1 = 4$ m, $H_2 = 2$ m, $L = 2.5$ m, and $t = 30$ ns.

schemes (OOK and PPM). This correlation is very well reproduced by a ceiling-bounce model for the impulse response. Rather than evaluating a candidate modulation scheme based on its performance on an ensemble of measured channels, one can instead use the uniform and reproducible method of evaluating performance for the ceiling-bounce impulse response. Using this ceiling-bounce model, we give a simple method for predicting power requirements given simple parameters of the room and the location of the transmitter and receiver.

APPENDIX

IMPULSE RESPONSE DUE TO AN INFINITE PLANE

Referring to Fig. 8, we define a coordinate system (x, y, z) where the positive z direction is "up." Let the transmitter be located at $(-L, 0, -H_1)$ and pointed toward the ceiling, and let the receiver be located at $(+L, 0, -H_2)$, with an active area A , and also pointed toward the ceiling. Hence, the distance of the transmitter to the ceiling is H_1 , and the distance of the receiver to the ceiling is H_2 . We define coordinates (x', y', z') so that the transmitter is located at $(-l, 0, 0)$ and the receiver is at $(+l, 0, 0)$ in the new coordinates, and so

$$l^2 = L^2 + \left(\frac{H_1 - H_2}{2} \right)^2. \tag{22}$$

Hence

$$\begin{pmatrix} x' \\ y' \\ z' \end{pmatrix} = \begin{pmatrix} \cos(\theta) & 0 & \sin(\theta) \\ 0 & 1 & 0 \\ -\sin(\theta) & 0 & \cos(\theta) \end{pmatrix} \begin{pmatrix} x \\ y \\ z \end{pmatrix} + \begin{pmatrix} H \sin(\theta) \\ 0 \\ H \cos(\theta) \end{pmatrix} \quad (23)$$

where we have defined

$$\theta = \arctan\left(\frac{H_1 - H_2}{2L}\right) \quad (24)$$

and

$$H = \frac{H_1 + H_2}{2}. \quad (25)$$

For light to travel from the transmitter to the receiver in less than time t via a single bounce, the position of the reflector must satisfy

$$V_t: \frac{(x')^2}{(ct/2)^2} + \frac{(y')^2}{(ct/2)^2 - l^2} + \frac{(z')^2}{(ct/2)^2 - l^2} < 1. \quad (26)$$

V_t is the interior of an ellipsoid with foci at the transmitter and receiver locations, and a major axis length of ct . Hence $V_t \cap P$ is the interior of the ellipse on the ceiling plane that contributes to the impulse response in the interval $[0, t)$ and is defined by

$$\begin{aligned} & \frac{(H \sin(\theta) + x \cos(\theta))^2}{(ct/2)^2} + \frac{y^2}{(ct/2)^2 - l^2} \\ & + \frac{(H \cos(\theta) - x \sin(\theta))^2}{(ct/2)^2 - l^2} < 1. \end{aligned} \quad (27)$$

Hence we can write

$$h(t) = \frac{d}{dt} \left[\int_{V_t \cap P} f(x, y) dA \right] \quad (28)$$

where, from [9], $f(x, y)$ is

$$\frac{\frac{\rho A}{\pi^2} H_1^2}{(H_1^2 + (x - l \cos(\theta))^2 + y^2)^2} \frac{H_2^2}{(H_2^2 + (x + l \cos(\theta))^2 + y^2)^2}. \quad (29)$$

In the general case, with no constraints on L, H_1 , or H_2 , numerical integration of (28) is required.

For the special case of $L = 0$ (i.e., the horizontal separation between the transmitter and receiver is zero), we can evaluate $h(t)$ explicitly. We have $V_t \cap P$ defined by

$$x^2 + y^2 < ((ct/2)^2 - H^2) \left(1 - \frac{l^2}{(ct/2)^2} \right) = g^2(t) \quad (30)$$

which defines the interior of a circle of radius $g(t)$, and

$$f(x, y) = \frac{\frac{\rho A}{\pi^2} H_1^2}{(H_1^2 + x^2 + y^2)^2} \frac{H_2^2}{(H_2^2 + x^2 + y^2)^2}. \quad (31)$$

Converting to polar coordinates (r, ϕ) in the (x, y) plane yields

$$\begin{aligned} h(t) &= \frac{\rho A}{\pi^2} \frac{d}{dt} \left[\int_0^{g(t)} \int_0^{2\pi} \frac{H_1^2 H_2^2 r}{(H_1^2 + r^2)^2 (H_2^2 + r^2)^2} d\phi dr \right] \\ &= \frac{2\rho A H_1^2 H_2^2}{\pi} \frac{d}{dt} \left[\int_0^{g(t)} \frac{r}{(H_1^2 + r^2)^2 (H_2^2 + r^2)^2} dr \right]. \end{aligned} \quad (32)$$

Applying the chain rule $(d/dt) \int_0^{g(t)} f(r) dr = f(g(t))g'(t)$ yields

$$\begin{aligned} h(t) &= \frac{\rho A H_1^2 H_2^2}{\pi} \frac{2g(t)g'(t)}{(H_1^2 + g^2(t))^2 (H_2^2 + g^2(t))^2} \\ &= \frac{\rho A H_1^2 H_2^2}{\pi} \frac{\frac{d}{dt}[g^2(t)]}{(H_1^2 + g^2(t))^2 (H_2^2 + g^2(t))^2} \end{aligned} \quad (33)$$

and substituting $g^2(t)$ from (30) gives

$$\begin{aligned} h(t) &= \frac{c\rho A H_1^2 H_2^2}{\pi} \frac{ct}{2} \left(1 - \frac{l^2 H^2}{(ct/2)^4} \right) u(t - 2H/c) \\ &\times \left[H_1^2 + \left(\left(\frac{ct}{2} \right)^2 - H^2 \right) \left(1 - \frac{l^2}{(ct/2)^2} \right) \right]^{-2} \\ &\times \left[H_2^2 + \left(\left(\frac{ct}{2} \right)^2 - H^2 \right) \left(1 - \frac{l^2}{(ct/2)^2} \right) \right]^{-2}. \end{aligned} \quad (34)$$

REFERENCES

- [1] J. M. Kahn, W. J. Krause, and J. B. Carruthers, "Experimental characterization of nondirected indoor infrared channels," *IEEE Trans. Commun.*, vol. 43, pp. 1613–1623, Feb./Mar./Apr. 1995.
- [2] H. Hashemi, G. Yun, M. Kavehrad, F. Behbahani, and P. Galko, "Indoor propagation measurements at infrared frequencies for wireless local area networks applications," *IEEE Trans. Veh. Technol.*, vol. 43, pp. 562–576, Aug. 1994.
- [3] J. R. Barry, J. M. Kahn, W. J. Krause, E. A. Lee, and D. G. Messerschmitt, "Simulation of multipath impulse response for indoor wireless optical channels," *IEEE J. Select. Areas Commun.*, vol. 11, pp. 367–379, Apr. 1993.
- [4] J. R. Barry, *Wireless Infrared Communications*. Boston, MA: Kluwer Academic, 1994.
- [5] H. Hashemi, "Impulse response modeling of indoor radio propagation channels," *IEEE J. Select. Areas Commun.*, vol. 11, pp. 967–978, Sept. 1993.
- [6] F. R. Gfeller and U. H. Bapst, "Wireless in-house data communication via diffuse infrared radiation," *Proc. IEEE*, vol. 67, pp. 1474–1486, Nov. 1979.
- [7] G. W. Marsh and J. M. Kahn, "Performance evaluation of experimental 50-Mb/s diffuse infrared wireless link using on-off keying with decision-feedback equalization," *IEEE Trans. Commun.*, vol. 44, pp. 1496–1504, Nov. 1996.
- [8] M. D. Audeh, J. M. Kahn, and J. R. Barry, "Performance of pulse-position modulation on measured nondirected indoor infrared channels," *IEEE Trans. Commun.*, vol. 44, pp. 654–659, June 1996.
- [9] M. D. Kotzin, "Short-Range Communications Using Diffusely Scattered Infrared Radiation," Ph.D. dissertation, Northwestern Univ., Evanston, IL, June 1981.



Jeffrey B. Carruthers (S'87–M'97) received the B.Eng. degree in computer systems engineering from Carleton University, Ottawa, Ont., Canada, in 1990, and the M.S. and Ph.D. degrees in electrical engineering from the University of California at Berkeley in 1993 and 1997, respectively.

He joined a SONET development group of Bell-Northern Research, Ottawa, in 1990. From 1992 to 1997, he was a Research Assistant at the University of California at Berkeley. He is currently an Assistant Professor of Electrical and Computer Engineering at Boston University, Boston, MA. His research interests are in broad-band wireless communications.

Dr. Carruthers is a member of the IEEE Communications and Social Implications of Technology Societies.

Joseph M. Kahn (M'87) received the A.B., M.A., and Ph.D. degrees in physics from the University of California, Berkeley (U.C. Berkeley), in 1981, 1983, and 1986, respectively. His Ph.D. thesis was entitled "Hydrogen-Related Acceptor Complexes in Germanium."

From 1987 to 1990, he was a Member of Technical Staff in the Lightwave Communications Research Department, AT&T Bell Laboratories, Crawford Hill Laboratory, Holmdel, NJ, where he performed research on multigigabit-per-second coherent optical fiber transmission systems and related device and subsystem technologies. He demonstrated the first BPSK-homodyne optical fiber transmission system and achieved world records for receiver sensitivity in multigigabit-per-second systems. He joined the faculty of U.C. Berkeley in 1990, where is currently a Professor with the Department of Electrical Engineering and Computer Sciences. His research interests include infrared and radio wireless communications and optical fiber communications.

Dr. Kahn is a recipient of the National Science Foundation Presidential Young Investigator Award and is a member of the IEEE Communications Society and IEEE Lasers and Electro-Optics Society. He is serving currently as a technical editor for IEEE PERSONAL COMMUNICATIONS MAGAZINE.